Superimposition of eye fundus images for longitudinal analysis from large public health databases

Guillaume Noyel, Rebecca Thomas, Gavin Bhakta, Andrew Crowder, David Owens, Peter Boyle

Superimposition of eye fundus images for longitudinal analysis from large public health databases

Guillaume Noyel[a]*, Rebecca Thomas[b], Gavin Bhakta[c], Andrew Crowder[c], David Owens[b], Peter Boyle[a,d]

[a] International Prevention Research Institute, 95 cours Lafayette, F-69006 Lyon, France.
[b] Diabetes Research Group, Institute of Life Sciences, College of Medicine, Swansea University, SA2 8PP, Wales, UK
[c] Diabetic Eye Screening Wales, 1 Fairway Court, Tonteg Road, Upper Boat, Treforest, Pontypridd CF37 5UA, Wales, UK
[d] Strathclyde Institute of Global Public Health, University of Strathclyde, Glasgow, UK.

*Corresponding author Guillaume Noyel.
Address: International Prevention Research Institute, 95 cours Lafayette, F-69006 Lyon, France. Tel.: +33 4 72 17 11 99 ; fax: +33 4 72 17 11 90. *E-mail address:* guillaume.noyel@i-pri.org
URL: http://www.i-pri.org/guillaume-noyel-research-director/

ABSTRACT:

In this paper, we present a method for superimposition (i.e. registration) of eye fundus images from persons with diabetes screened over many years for Diabetic Retinopathy. The method is fully automatic and robust to camera changes and colour variations across the images both in space and time. All the stages of the process are designed for longitudinal analysis of cohort public health databases. The method relies on a model correcting two radial distortions and an affine transformation between pairs of images which is robustly fitted on salient points. Each stage involves linear estimators followed by non-linear optimisation. The model of image warping is also invertible for fast computation. The method has been validated 1. on a simulated montage with an average error of 0.81 pixels for one distortion (respectively 1.08 pixels for two distortions) and a standard deviation of 1.36 pixels (resp. 3.09) in images of 1568 x 2352 pixels in both directions and 2 on public health databases with 69 patients with high quality images (with 271 pairs and 268 pairs) with a success rates of 96 % and 97 % and 5 patients (with 20 pairs) with low quality images with a success rate of 100%.

Keywords: eye fundus images, image registration, radial distortion, invertible model, longitudinal analysis, public health databases

1 Introduction

Diabetic Retinopathy (DR) is one of the major causes of visual impairment in the world and therefore represents a major public health challenge. It is a complication of both types of diabetes mellitus, which affects the light perception part of the eye (retina). DR may lead to the development of sight threatening lesions and without adequate and timely treatment the patient could lose their sight and eventually become blind (International Diabetes Federation and The Fred Hollows Foundation, 2015) (Scanlon et al., 2009). DR is often asymptomatic until an advanced stage, thereby screening to detect sight threatening DR at an early stage is essential which has resulted in the introduction of DR Screening services in many countries such as UK (Harding et al., 2003), USA, the Netherlands, France, etc. The commonest screening method involves acquiring eye fundus images on an annual or biennial basis.

As these DR screening programs have been in existence over several years, performing longitudinal analysis of the eye fundus images of the same patient is now possible. However, in order to accurately compare the evolution of DR over time, the images must be perfectly super-imposed.

The direct superimposition of two images of the same patient never gives good results (see **Fig. 1**). Indeed, for two separate photographic-eye examinations the patient is never in exactly in same

position and also the camera may differ. Therefore, the super-imposition method has to take into account the different causes of the deformation such as:

- The position of the patient: by taking into account rotation, translation and scaling.
- The change of the camera: by using scaling.
- The projection of a 3D scene assimilated to a sphere (the retina of the eye) onto the 2D plane of the sensor of the camera: by using a radial correction process.
- The radial deformation due to the optics of the camera: by using a radial correction process.
- The colour variability between images due to the light intensity and sensor.

To perform a superimposition - also named registration – two stages are regarded as necessary: a model of deformation and a matching criterion to fit the model. There are several models in existence to allow super-imposition between pairs of eye fundus images. The earliest methods relied on fluorescein images and based on a composition of translation, rotation and scaling - i.e. an affine transformation model (Zana and Klein, 1999a, b). The bifurcations of the vessels were used to match the points and fit the model. Another matching criterion consists in the minimisation of image intensity differences (Adal et al., 2014; Cideciyan, 1995; Matsopoulos et al., 1999; Ritter et al., 1999).

Other methods are based on similarity (i.e. a rotation and a translation) and an elastic model of deformation (Fang and Tang, 2006; You et al., 2005).

More recently, it has been shown that a quadratic model gives better registration results (Adal et al., 2014; Can et al., 2002; Chanwimaluang et al., 2006; Stewart et al., 2003). The difficulty inherent in these models is to estimate their parameters. To overcome such a limitation, a radial distortion model has been introduced by Lee et al. (2007) and compared to previous methods in Lee et al. (2010). It consists of adding a radial model to the affine transformation in order to correct the effects of radial distortion due to the geometry of the camera and of the eye. However, the superimposition of eye fundus images is performed with images acquired by the same camera during the same examination. However, superimposing images acquired at different times by different cameras in large databases still remains a challenging problem.

In this paper, our contribution has been to address this challenge by presenting a robust superimposition method designed for longitudinal screening of large public health image based databases.

Therefore, after presenting a complete method to superimpose pairs of images, we will present a quality check of the registration and finally, validation of our methodology using different patient databases.

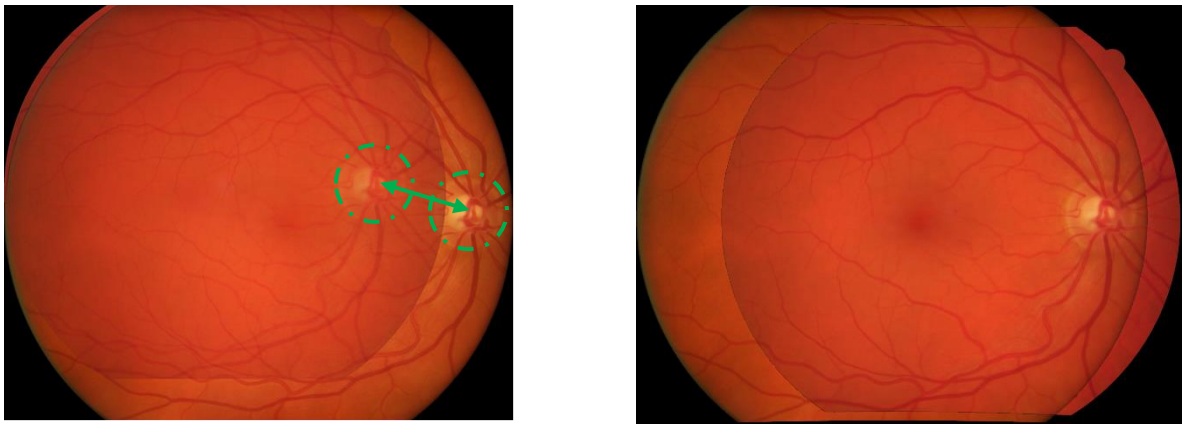

(a) Naive superimposition of images

(b) Perfect superimposition of images by using a model

Fig. 1 Superimposition of eye fundus images

2 Methods

During a photographic eye examination, eye fundus (retina) two images of both eyes are acquired i.e. a 45 degree “nasal” and “macular” field (**Fig. 3**). The aim of this study was to develop robust algorithms for superimposition of images in the same positions while being captured during two different exams and often with different cameras and resolutions. Our aim was not to develop large mosaics of eye fundus images acquired during the same examination with the same camera (Chanwimaluang et al., 2006), but to propose a robust method for longitudinal studies involving large databases with images acquired in heterogeneous conditions. Therefore, we have paid particular attention to the development of robust and fast algorithms for longitudinal screening.

Our method is based on a pre-processing stage consisting of (1) normalising the colour of the eye fundus image (Noyel et al., 2015), (2) the extraction of characteristic points in pairs of images, (3) a matching procedure, (4) the use of a model correcting radial distortion of both images and (5) the estimation of the parameters of the model by a robust optimisation. The method is validated (6) on a simulated montage and the superimpositions of the image of the database are verified (7).

A schematic description of the study is represented in **Fig. 2**. The different stages have been designed to provide efficient solutions to the superimposition of images acquired for practical screening. Between two examinations, the camera might have been changed producing differences in colour, resolution and radial distortion between images. Moreover, we will show that our method is efficient both on high quality images acquired following pupillary dilation and low quality images without dilatation of the pupils prior to photography.

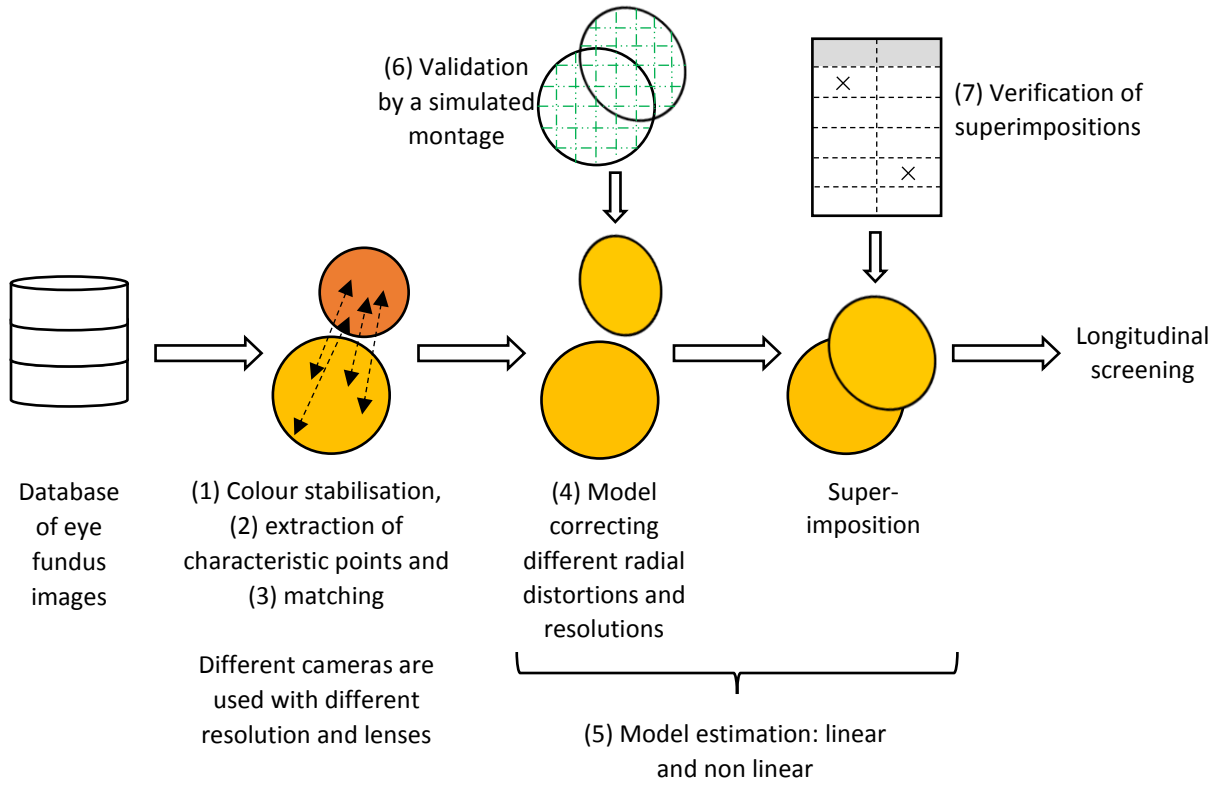

Fig. 2 Framework of eye fundus superimposition of images for longitudinal screening. After colour stabilisation (pre-processing) and extraction of characteristic points, the points are matched and the model is estimated. The differences are corrected in term of radial distortions and resolutions between the images

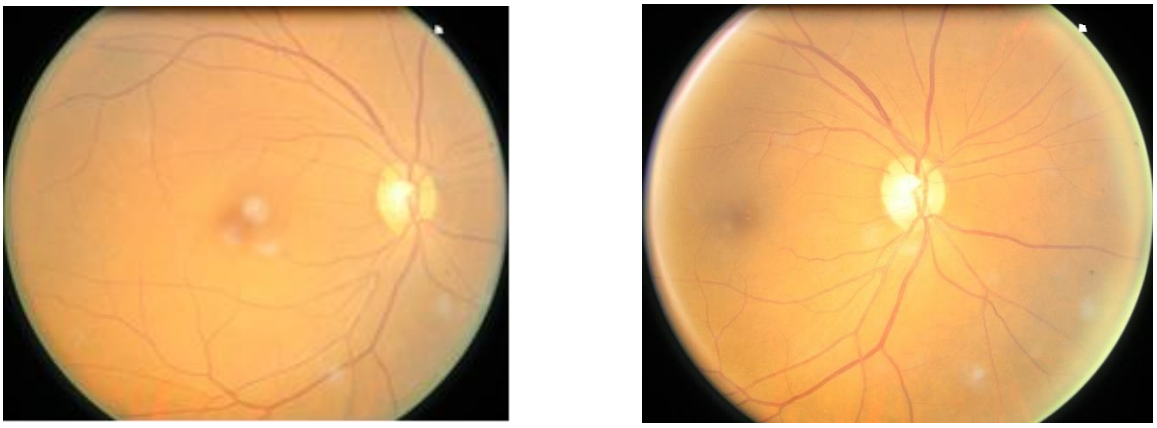

(a) Macular view (b) Nasal view

Fig. 3 Macular and nasal view of an eye fundus acquired without pupil dilation and in harsh conditions

2.1 Extraction of characteristic points

The brightness of eye fundus images is non-uniform due to various reasons: disease such as cataract, motion of the patient, acquisition conditions and differences in absorptions of the light in the eye (Walter, 2003; Walter and Klein, 2005). Some parts of the images appear as bright while others are dark. Moreover, the possible change of the eye fundus camera between two separate examinations may contribute to a change in the colour between two images of the same eye (**Fig. 4**).

We have used a method (Noyel et al., 2015) to correct the variations of colour contrast between the images. Results can be seen in **Fig. 4**.

This is then followed by the extraction of several salient points (**Fig. 5**) using the Scale-Invariant Feature Transform - SIFT - algorithm (Lowe, 2004; Vedaldi and Fulkerson, 2008). The SIFT algorithm has been designed to be robust to the variation of observation angle and to some variations in lightning. Briefly SIFT consists of extracting key points based on a multiscale analysis. Then series of descriptors are computed for each salient point. These descriptors are used for point matching

A similar detector, the SURF (Speeded Up Robust Features) detector, was previously used for eye fundus image superimposition (Cattin et al., 2006).

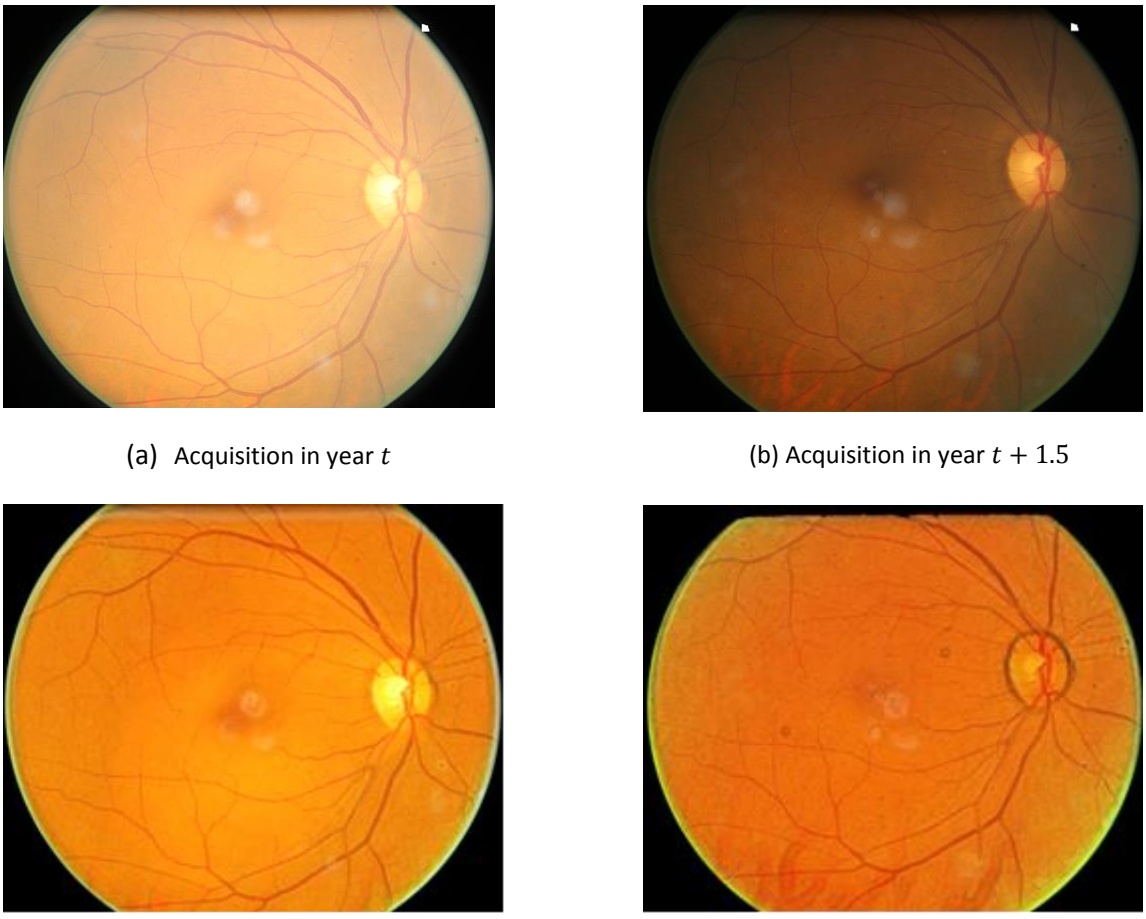

(a) Acquisition in year t

(b) Acquisition in year $t + 1.5$

(c) Acquisition in year t after colour correction

(d) Acquisition in year $t + 1.5$ after colour correction

Fig. 4 (a), (c) Eye fundus images of the same patient acquired during two exams with 1.5 years of interval. (b), (d) Colour stabilisation of eye fundus images with a low quality.

2.2 Point matching

As point matching with Lowe's method (Lowe, 2004) is not robust enough to estimate the rotation on our database, we have created a three-step procedure:

(a) A first matching by Lowe's method followed by a refined selection of the correspondence vectors according to their size and orientation
(b) An estimate of the homography using the algorithm of section 2.4.1. The position of the key points is modified according to the homography.
(c) Step (a) is applied a second time using the transformed points.

After this first matching, one image is put on the right while the other on the left after resizing and padding to have the same size (**Fig. 5**). As some points are incorrectly matched, some correspondences vectors v between matched points are inconsistent. A two-step selection is performed using their lengths l and orientations θ:

1) only the vectors v whose length l_v and orientation θ_v is in the interval $\{|l_v - E\{l_v\}| \leq \sigma\{l_v\}\ and\ |\theta_v - E\{\theta_v\}| \leq 5°\}$. $E\{\}$ is the mean and $\sigma\{\}$ the standard deviation of a variable.
2) Among the selected vectors $\tilde{v}$, only the vectors whose length $l_{\tilde{v}}$ and orientation $\theta_{\tilde{v}}$ is in the interval $\{|l_{\tilde{v}} - E\{l_{\tilde{v}}\}| \leq \max(3\sigma\{l_{\tilde{v}}\}, 5\% \times ysize)\ \ and\ |\theta_{\tilde{v}} - E\{\theta_{\tilde{v}}\}| \leq \max(5°, \sigma\{\theta_{\tilde{v}}\})\}$ $ysize$ is the number of lines in the image.

After matching the points, a model of transformation is estimated.

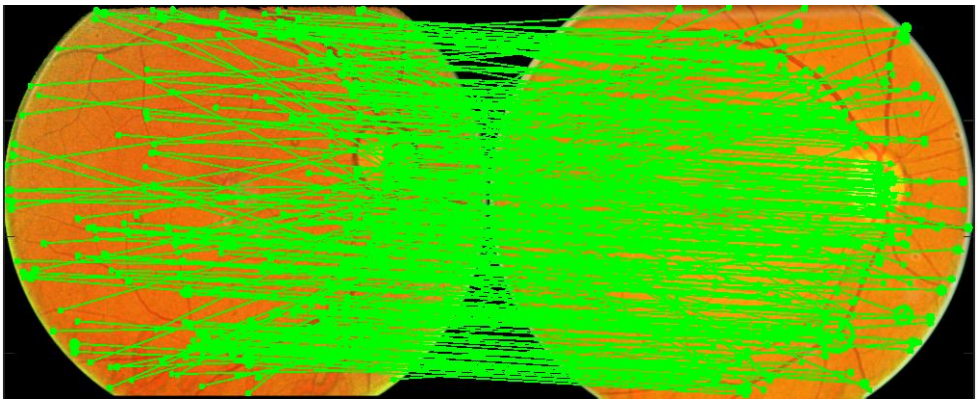

(a) Initial matching

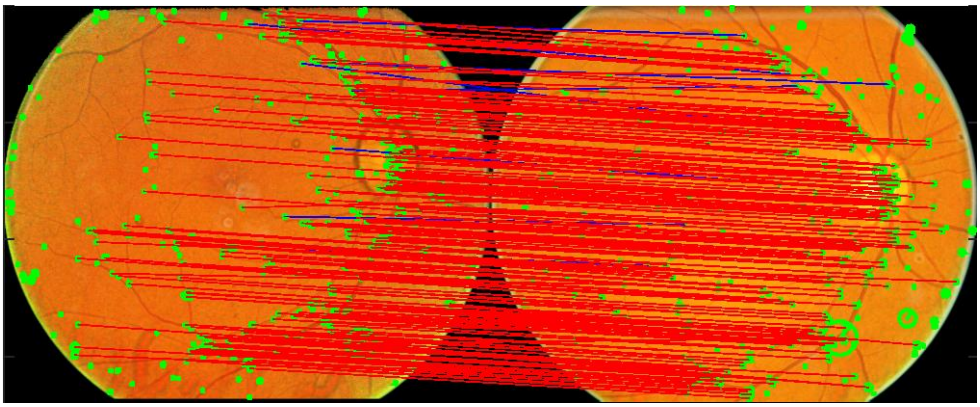

(b) Matching after first simplification (in red and in blue) and after second simplification (in blue)

Fig. 5 Point extraction and matching between images

2.3 Model of deformation

The model of deformation ensures a correct superimposition between the images. Several deformations are taken into account: (i) the difference in terms of positions of the eye between a pair of images will be corrected by an affine transformation (i.e. and homography) and (ii) the radial deformations due to the projection of the eye into the camera and due to the optics of the camera (Hartley and Zisserman, 2004) will be corrected using a radial transformation.

Lee et al. (2007, 2008) have proposed a model coupling a unique radial transformation for both images and a homography. Lee et al. (2010) have made the comparison with two other second order models.

In this paper, as we were interested in analysing images of patients acquired during exams with an approximate one year interval, we extended their approach by defining a model with one homography H and two radial distortions, i.e. one for each image. Indeed, the camera may have changed between screening exams on a large number of patients.

The affine homography H is defined as:

$$H = \begin{bmatrix} A & T \\ O^T & 1 \end{bmatrix} = \begin{bmatrix} a_{11} & a_{12} & t_x \\ a_{21} & a_{22} & t_y \\ 0 & 0 & 1 \end{bmatrix} \quad (1)$$

$A = \begin{bmatrix} a_{11} & a_{12} \\ a_{21} & a_{22} \end{bmatrix}$ is an affine transformation, $\forall i,j \in [1 \dots 2], a_{ij} \in \mathbb{R}$, and $T = \begin{bmatrix} t_x \\ t_y \end{bmatrix}$, $t_x, t_y \in \mathbb{R}$, is a translation.

The radial distortion due the background of the sphere surface of the eye and of the radial distortion of the camera was modelled by a *division model* (Fitzgibbon, 2001) in the following way:

$$\bar{P}^d = (1 + k(r^d)^2).\bar{P}^u \quad (2)$$

with:

- $P^d \in \mathbb{R}^2$ the distorted coordinates in the original (i.e. distorted) image
- $P^u \in \mathbb{R}^2$ the undistorted coordinates in the undistorted image
- $\bar{P}^d \in \mathbb{R}^2$ the distorted coordinates centred on the image centre *c*: $\bar{P}^d = P^d - c$
- $\bar{P}^u \in \mathbb{R}^2$ the undistorted coordinates centred on the image centre *c*: $\bar{P}^u = P^u - c$
- $r^d = \left\|P^d - c\right\| = \left\|\bar{P}^d\right\| \in \mathbb{R}$, the distance of the deformed coordinates P^d from the optic centre *c* (i.e. the image centre).
- k a real parameter of distortion in $[-0.2 ; 0.2]$, after normalisation by $(1 + \|c\|)^2$.

The model was named *division model* because the distorted coordinates were divided by the radial distortion $\bar{P}^d/(1 + k(r^d)^2) = \bar{P}^u$.

The distorted image corresponds to the original image and the undistorted image is the image after the correction of radial distortion.

Given P_1^d and P_2^d the coordinates of the points in the original (i.e. deformed) images 1 and 2, k_1 and k_2 the distortion parameters, $c_1$and c_2 the image centres, the model mapping image 1 into image 2 is defined as follows:

$$\frac{\bar{P}_2^d}{(1 + k_1(r_2^d)^2)} + c_2 = H\left[\frac{\bar{P}_1^d}{(1 + k_2(r_1^d)^2)} + c_1\right] \quad (3)$$

If the camera used to acquire both images is the same, the distortion parameters are equal $k_1 = k_2$, and the model corresponds to the model of Lee et al. (2007).

The model is estimated after having extracted and matched the points in the pair of original images (target and reference). Therefore, the radial distortion correction is performed after the detection of the feature correspondence points in the original (i.e. distorted) image. It has been programmed in the subsequent way.

2.4 Estimation of the model parameters

The parameters of the model are estimated by a different method of Lee et al. (2007). Indeed, the radial distortion is estimated after the homography without needing any estimation by a preliminary calibration of the camera (Hartley and Zisserman, 2004). Moreover, we have conceived linear initialisers at each step of the optimisation of the model (**Fig. 6**).

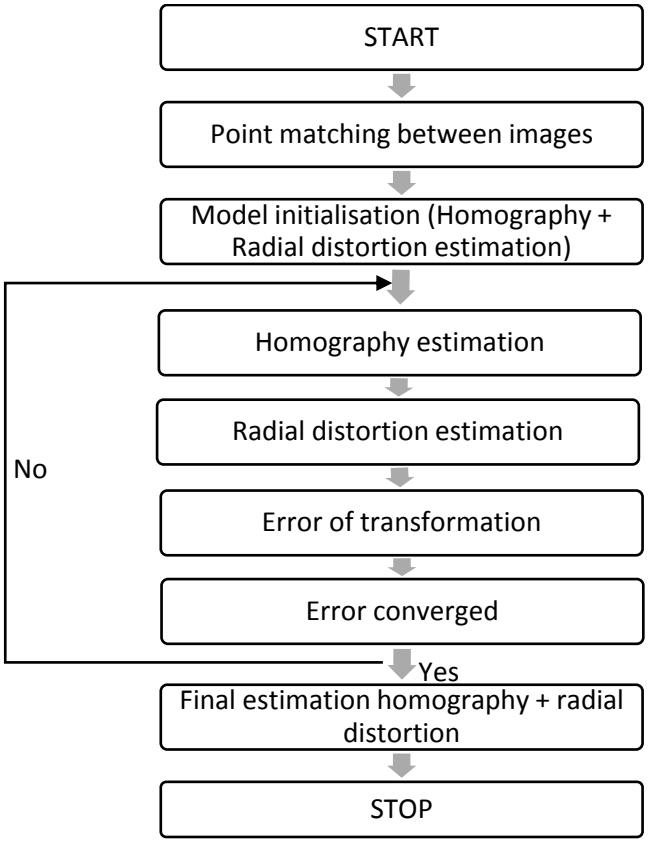

Fig. 6 Flowchart of the superimposition method based on homography and radial distortion

2.4.1 Estimation of the homography

An affine homography can be decomposed according to the following scheme (Hartley and Zisserman, 2004):

$$A = R(\theta)R(-\phi)DR(\phi) \tag{4}$$

$R(\theta)$ and $R(\phi)$ are rotation matrices of angle θ and ϕ respectively and D is a diagonal matrix:

$$D = \begin{pmatrix} \lambda_1 & 0 \\ 0 & \lambda_2 \end{pmatrix}$$

λ_1 and λ_2 are two scaling values. The matrix A is a composition of a rotation by ϕ, a scaling by λ_1(respectively λ_2) in x (respectively y) direction, a rotation by $-\phi$ and then another rotation by θ. The decomposition is obtained using the Singular Value Decomposition (SVD) method.

The estimation of an homography is basically performed using the "gold standard" algorithm of Hartley and Zisserman (2004). However, as there is also a radial distortion in the image, the deformation is not entirely modelled by a homography. Therefore, some homographies must be discarded. In particular, those with a scaling factor on the x and y axis with a relative difference greater than 1%. For this purpose, several estimates (until 50) using the gold standard algorithm are performed if the relative difference between the scaling factors is greater than 1%. If the value of 1% is never reached, then the homography with the smallest relative difference between the scaling factors is kept.

2.4.2 Estimation of the model with one radial distortion

When the camera is the same for both images, only one radial distortion needs to be estimated.

In the flowchart of **Fig. 6**, the convergence criteria becomes

$$convergence = [l_{err}(n) < \varepsilon] \; and \left[\frac{l_{err}(n) - l_{err}(n-1)}{l_{err}(n-1)} < tol\right] \; and \; [n < MaxIter]$$

l_{err} is the list of errors at each iteration n, $\varepsilon = 0.01$ is the tolerance on the error, $tol = 0.01$ is a tolerance on the relative error between iterations and $MaxIter = 100$ is the maximum number of iterations.

Linear estimators are used at each step of the parameter estimation. The final optimisation is performed with a linear estimator followed by a non-linear optimiser such as Levenberg-Marquardt (Bonnans et al., 2006; More, 1977).

We will now present the linear estimators.

2.4.2.1 Linear estimator of the radial distortion parameter k

Using equations **(1)** and (**3**), the following equation is obtained:

$$\frac{\bar{P}_2^d}{(1 + k(r_2^d)^2)} + c_2 = A\left[\frac{\bar{P}_1^d}{(1 + k(r_1^d)^2)} + c_1\right] + T \tag{5}$$

A is the matrix of the affine transformation and T is the vector of translation.
Equation (**5**) implies that:

$$k^2[(r_1^d r_2^d)^2 . d] + k\left[\left(r_1^{d\,2} + r_2^{d\,2}\right).d + r_1^{d\,2}.P_2 - r_2^{d\,2}.AP_1\right] = -[P_2 + d - AP_1] \tag{6}$$

with $d = c_2 - Ac_1 - T$.
Equation (**6**) is a linear equation in k when H (i.e. A and T) is known. k is determined using least squares algorithm.

2.4.2.2 Linear estimator of the homography H and of the radial distortion parameter k

Using equation (**5**) the following equation is determined:

$$\begin{array}{ccccccccc} k^2 d[(r_1^d r_2^d)^2] & +kd\left[r_1^{d\,2} + r_2^{d\,2}\right] & +k\left[r_1^{d\,2}.P_2\right] & -kA\left[r_2^{d\,2}.P_1\right] & -A[P_1] & +d[1] & = & -[P_2] \\ k^2 d[M_1] & +kd[M_2] & +k[M_3] & -kA[M_4] & -A[M_5] & +d[M_6] & = & -[M_7] \end{array} \tag{7}$$

Equation (**7**) is a linear equation with variables M_i. k and H (with the intermediate of A and d) are determined using least squares estimate.

2.4.3 Estimation of the model with two radial distortions

When a different camera is used for the pair of images, two radial distortions must be estimated.

In the flowchart of **Fig. 6**, the convergence criteria becomes:

$$convergence = [l_{err}(n) < \varepsilon] \; and \; \left[\frac{l_{err}(n) - l_{err}(n-1)}{l_{err}(n-1)} < tol\right] \; and \; [k_1 and \; k_2 \in [-0.2\,;0.2]]$$
$$and \; [n < MaxIter]$$

The same parameters l_{err}, n, $\varepsilon = 0.01$, $tol = 0.01$, $MaxIter = 100$ are used for the estimation of both distortions.

For each estimate, the radial distortion parameters must be in the interval $[-0.2\,;0.2]$. If not, the algorithms stop and the model estimate with the smallest error is selected.

As previously, linear estimators are used at each step of the parameter estimation. The final optimisation is followed by a non-linear optimiser such as trust region method (Bonnans et al., 2006; Moré, 1983) with bounds $[-0.2\,;0.2]$ for the radial distortion parameters.

We will now present the linear estimators.

2.4.3.1 Linear estimator of the radial distortion parameters k_1 and k_2

Equation (**3**) gives the following equation:

$$\frac{\bar{P}_2^d}{(1 + k_2(r_2^d)^2)} + c_2 = A\left[\frac{\bar{P}_1^d}{(1 + k_1(r_1^d)^2)} + c_1\right] + T \tag{8}$$

Equation (**8**) implies that:

$$k_1 k_2[(r_1^d r_2^d)^2.d] + k_1\left[r_1^{d\,2}.d + r_1^{d\,2}.P_2\right] + k_2\left[r_2^{d\,2}.d - r_2^{d\,2}.AP_1\right] = -[P_2 + d - AP_1] \tag{9}$$

with $d = c_2 - Ac_1 - T$.

Equation (**9**) is a linear equation in k_1 and k_2 when H (composed of A and d) is known. k_1 and k_2 are determined using least squares method.

2.4.3.2 Linear estimator of the radial distortion parameters k_1 and k_2 and the homography

From equation (**3**), the following one is obtained:

$$\begin{array}{ccccccccc} k_1k_2d[(r_1^dr_2^d)^2] & +k_1d\left[r_1^{d\,2}\right] & +k_1\left[r_1^{d\,2}.P_2\right] & +k_2d\left[r_2^{d\,2}\right] & -k_2A\left[r_2^{d\,2}.P_1\right] & -A[P_1] & +d[1] & = -[P_2] \\ k_1k_2d[M_1] & +k_1d[M_2] & +k_1[M_3] & +k_2d[M_4] & -k_2A[M_5] & -A[M_6] & +d[M_7] & = -[M_8] \end{array} \tag{10}$$

Equation (**10**) is a linear equation with variables M_i. k_1, k_2 and H (with the intermediate of A and d) are determined using least squares algorithm.

2.5 Image warping

In order to analyse a large database, a fast algorithm of image warping is needed. Forward warping is time consuming and so we therefore use inverse warping. However, the registration model needs to be invertible (Wolberg, 1990).

The radial distortion is modelled in equation (**3**) by a *division model* (Fitzgibbon, 2001). Wonpil (2003) and Park et al. (2009) have computed an approximate transformation for a standard distortion method. Here, we compute the inversion of the *division model*.

Given $r^u = \|P^u - c\| = \|\bar{P}^u\| \in \mathbb{R}$, the distance of the undistorted coordinates P^c from the optic centre c, using equation (**3**), we have:

$$r^d = (1 + k(r^d)^2).r^u \tag{11}$$

Equations (**3**) and (**11**), implies that:

$$\bar{P}^u = \frac{r^u}{r^d}\bar{P}^d = W^{-1}(\bar{P}^d) \tag{12}$$

In order to use invert warping, it is necessary to determine $W^{-1}$the undistorted points P^u knowing P^d. From equation (**12**), it is equivalent to determine r^u knowing r^d.

Equation (**11**) is equivalent to: $kr^u{r^d}^2 - r^d + r^u = 0$, which is a second order equation in r^d.

Its discriminant is equal to: $\Delta = 1 - 4k{r^u}^2$ with $\Delta > 0$. Its roots are $r^d = \frac{1 \pm \sqrt{1-4k{r^u}^2}}{2kr^u}$.

The inverse transformation W^{-1} corresponds to the root:

$$\mathrm{r^d = W^{-1}(r^u) = \frac{1 + \sqrt{1 - 4k{r^u}^2}}{2kr^u}} \tag{13}$$

Therefore, the transformation used is invertible. An invertible image warping method compared to a non-invertible method reduces the time from about 10 minutes to a few seconds on a standard computer using Matlab (16Go RAM, processor Intel i7-4702HQ, **2**.20GHz).

In **Fig. 2** and in **Fig. 7**, the results of superimposition with the radial distortion model are shown. One can notice the good quality of the superimposition. In the next section we will evaluate the quality of superimposition.

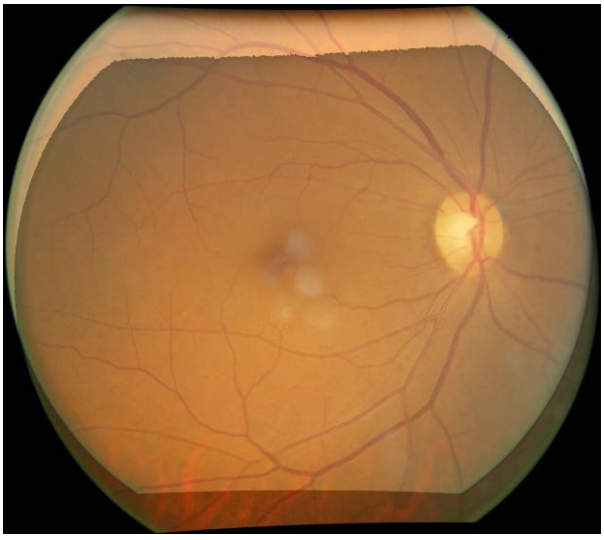

Fig. 7 Superimposition of a pair of eye fundus images with correction of two radial distortions

3 Experimental

The quality of image superimposition was evaluated through a simulated montage and using a database of patients. This latest validation is important as our method has been designed to analyse large public health image databases.

3.1 Validation by a simulated montage

We have created a montage by superimposing two eye fundus images and deforming them according to the methods presented by Lee et al. (2010). We have taken real images registered with an overlap percentage of 80% corresponding to the case that we have in a longitudinal database. No modification of colour was done to the images. After adding equally spaced landmarks, we have cut and deformed the images according to the model of Lee et al. (2010).

An affine transformation has been used, with rotation scaling and shearing. Then the image has been modified by a projective distortion. The radius of the eye ball has been approximated by the ratio between the radius of the disk of the image divided by the observation angle of the camera (45 degrees).

Then we have registered the images and measured the error between the landmarks after registration and their true position. With a single distortion, we have obtained a mean registration error of 0.81 pixels (standard deviation 1.36 pixels) in images of size 1568 x 2352 pixels (**Fig. 8**) with vessels of maximum diameter greater than of 30 pixels. The relative error respective to the image is 0.05%, and respective to the vessels is 2.7 %. With two distortions, the mean registration error is of 1.08 pixels (standard deviation 3.09 pixels) and the relative error is 0.07 % respective to the image and 3.6 % respective to the vessels. The error is mainly located on the external part of the superimposed image.

Such results demonstrate that the method gives a superimposition without noticeable difference. Therefore, this approach is suitable to perform an analysis in a large database.

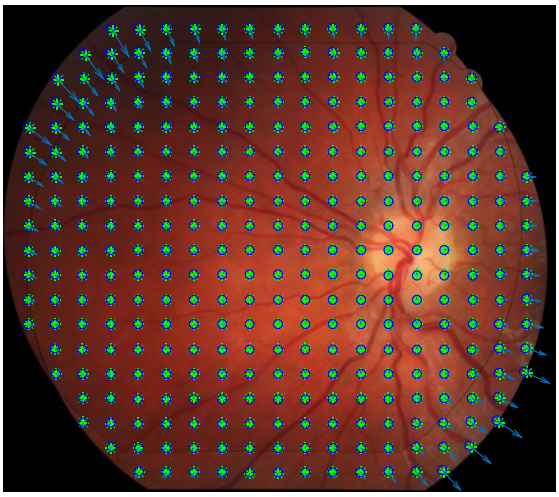

Fig. 8 Validation of the superimposition model by registering a pair of images previously deformed. The green points corresponds to the points of the reference image and the blue points to the points of the current image. The arrows represent the registration errors between the two images.

3.2 Validation with a public health database

In order to assess the evolution of Diabetic Retinopathy several screening programs in the world are in existence. Among them, in the United Kingdom, in Wales, the Diabetic Eye Screening Wales (DESW) has developed a program to screen the whole population with diabetes over the age of 12 years old. The programme has been in existence for just over 10 years at a national level and several thousands of patients have been screened annually for five or more years (Thomas et al., 2012).

We have performed trials of a database of 69 patients coming from the DESW. For each patient we have kept two series of two examinations with an approximate screening interval of one year between the examination events. For each event exam, four images are available, two positions (nasal and macular) for each eye. There were two series of images, with the first series are made up of 271 pairs of sufficient image quality and the second series included of 268 pairs. For each position, we have performed the superimposition of the images between the two different examinations. For all pairs of images the superimposition has been visually checked.

In first series of 271 pairs, 2 pairs have small differences in the external part of the superimposition. These differences are of the size of the diameter of a vessel. When the percentage of overlapping surface is low (around 30 %) compared to the surface of the superimposed image, we have noticed differences of the size of 1 vessel on 8 pairs of images. Therefore, the superimposition was successful for 96 % of the pairs and 99% if we consider the pairs in the same position.

In the second series of 268 pairs of images acquired a few years later, there are 6 images with a small difference (i.e. less than 1 vessel diameter). The superimposition was successful for 98 % of the pairs. However, in these images the central part was perfectly superimposed. We have developed another algorithm using, in addition to the matched points, the distance between the retinal vessels. This algorithm similar to those described by Can et al. (2002) and Lee et al. (2010) solves the registration problem for the images with a small overlapping area. These findings will be presented in a future paper.

In the pairs with a sufficient overlap, no noticeable difference has been perceived between them. This means that our method is suitable to be applied to analyse large databases.

As a second validation test, we have performed superimposition of images of low/poor quality for 5 patients. The acquisitions conditions were significantly harsher compared to the high quality images and the quality of images was quite heterogeneous in part due to the lack of pupillary dilatation prior to photography. The quality of image superimposition has been checked for the 20 pairs of images and in each case there was no noticeable difference in the superimposition, even on the border of the images.

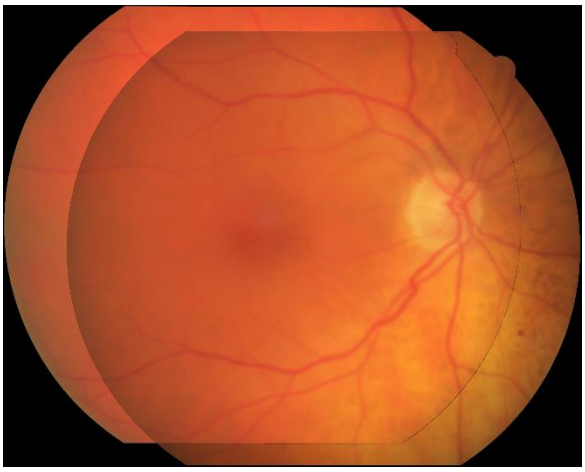

(a) Good superimposition

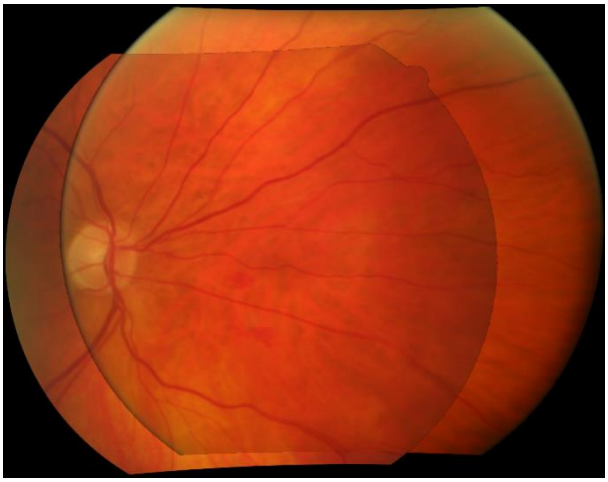

(b) Superimposition with small differences

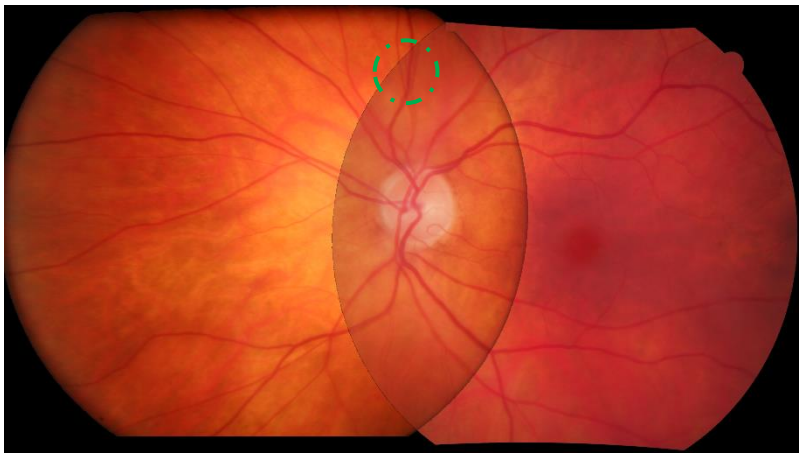

(c) Superimposition with small differences and a small overlap

Fig. 9 Examples of superimposition

4 Discussion

A robust method for the superimposition of fundus (retinal) images coming from a large database has been presented. It corrects the errors coming from the different position of the patient during image acquisition, the change in the camera employed (resolution and optical lenses), the projection of a 3D scene onto a plane and the variability of colour between images. The novelty of our method is to deal with eye fundus images acquired with different cameras (i.e. different resolutions and different lenses) and to be robust to strong colour variations between the images (Noyel et al., 2015). Our method has been designed to analyse large cohorts of patients' eye fundus images (i.e. examinations across time). Therefore, it goes further than the previous approaches (Adal et al., 2014; Can et al., 2002; Lee et al., 2010).

In our method, the registration model takes into account two radial distortions (one for each image) and a rotation, a translation and two scalings. The registration model is estimated based on images after colour stabilisation (Noyel et al., 2015). SIFT points are extracted and matched. Using these

points, the registration model is estimated by an iterative process of numerical optimisation. For each step, the parameters are estimated by linear estimators followed by a nonlinear estimation process.

The image warping is performed using a *division model* which is invertible and fast.

The accuracy of the superimposition method has been validated on a simulation montage. The superimposition error is in average 0.81 pixels for one distortion (respectively 1.08 for two distortions), the standard deviation is 1.36 pixels (resp. 3.09). The relative error respective to the image is 0.05% (resp. 0.07%), and respective to the vessels is 2.7 % (resp. 3.6%).

In order to assess the efficiency of our method for public health purposes, the superimposition method has been validated on public health databases with high quality images of 69 patients (two series including 271 pairs and 268 different pairs) and 5 patients with low quality images. In each case, there is no noticeable difference in the superimposed images if the overlap is sufficient (more than 50 % about). The superposition is successful in 96%, 97% and 100 % of the cases respectively. Moreover, the interest of the superimposition is to compare the evolutions in a public health database over many years. This is only useful when the image overlap is large enough. Therefore, our method is well suited for this purpose.

For images with a smaller overlap (e.g. 30% of the surface of the mosaic image), the superimposition may present small differences on the external part. To address this issue, we have developed another algorithm using in addition to the matched points, the distance between the vessels. It will be presented in a future paper.

In addition, our method could be useful for automatic detection of referral patients due to Diabetic Retinopathy (Abramoff et al., 2013; Decencière et al., 2013; Fleming et al., 2010; Quellec et al., 2016).

5 Conclusions

We have therefore successfully achieved a new method to superimpose eye fundus images coming from large public health databases. In addition to the previously existing methods, ours has been designed to deal with changes in terms of camera, lens, image resolution and colour between two exams of the same patient.

The method presented consists of fitting a registration model composed of a homography and two radial distortions on salient points extracted in images after colour stabilisation. The method is easy to use and does not require to extract intrinsic characteristics of the image such as the vessels or their branch points.

All the stages of the method have been designed to be robust and fast on heterogeneous databases. In particular, the equation of linear estimators of the parameters have been provided and an invertible model has been used to warp the images.

Our method has been validated on a montage and on public health databases of eye fundus exams of patients. Some patients had high quality images while other had images of lower quality due to differences in the conditions of acquisition. However, the results show that there is no noticeable difference between the images from two examinations with the eye in the same position (nasal or macular). The superimposition is correct in more than 96% of the cases.

In the future, we plan to develop an algorithm to perfectly superimpose eye fundus images acquired in two different positions with a small overlap and with different cameras.

6 Vitae

Guillaume Noyel is a research director at the International Prevention Research Institute where he is leading a project in Diabetic Retinopathy. He obtained a MSc from CPE-Lyon, France. He received his PhD in Mathematical Morphology from Mines ParisTech, Paris, in 2008 before working as a researcher in image processing at the Michelin Research Centre for 6 years. His principal fields of expertise are colour and multivariate image analysis, mathematical morphology, 3D image reconstruction for biomedical and industrial applications. He has been published in several journals and has obtained several international patents (EU, USA, China, and Japan) in these fields.

Rebecca Thomas is a postdoc diabetic retinopathy research officer within the Welsh Government funded diabetes research unit, Cymru at Swansea University, medical school. Prior to her PhD she was a senior retinal grader at the diabetic retinopathy screening service for Wales. She obtained her PhD from Cardiff University in 2015 with the topic being the epidemiology of diabetic retinopathy and an assessment of screening intervals. Her thesis has resulted in several high impact publications and further research grants. She has also been involved in the set up and development of screening services in Countries such as Mauritius and Trinidad.

Gavin Bhakta is the IT Systems Manager for Diabetic Eye Screening Wales (DESW), a national screening service which is part of Public Health Wales. He holds a BSc (Hons.) Computer Science and is the lead on the development of all communication and information systems for the service. Working collaboratively with the Diabetes Research Unit Cymru, he has contributed to the research programme by providing data which has been used in several significant publications. He has also been both lead and co-author on abstracts and poster presentations, focussing on operational planning and modelling.

Andrew Crowder is the Head of Programme for the Diabetic Eye Screening Wales (DESW). He qualified as a Biomedical Scientist in Haematology in Liverpool and moved to the NHS laboratories in Cardiff in 1985, after gaining a Fellowship of the Institute of Biomedical Science. After adding a Diploma in Healthcare Management, he moved into general NHS management in 2000, managing the Laboratory Medicine and Genetics Directorates. In 2011 he joined DESW and during his tenure has promoted a much higher level of involvement of DESW in research and has been personally involved in a number of studies.

Professor Owens CBE MD FRCP, Emeritus Professor of Diabetes at Cardiff University, and Professor of Diabetes Swansea University's College of Medicine. He has been involved in the research and the management of diabetes for more than 35years. He introduced the first community wide National Diabetic Retinopathy Screening Service for Wales in 2002. He is involved in introducing Retinopathy Screening services in other countries. He has collaborations with iPRI, Lyon. He is a member of the Association of Physicians of Great Britain and Ireland and is a Fellow of the Royal College of Physicians. He has published about 450 articles.

Professor Peter Boyle is BSc, PhD and DSc (Med) from the University of Glasgow, Faculty of Medicine. He is the president of the International Prevention Research Institute. He is an epidemiologist and an internationally cancer prevention advocate (The EU Code against Cancer, the European Tobacco Products Directive or the Globalisation of Cancer). He has published widely in the scientific and medical literature, including books and cancer atlases. He is a past Director of the WHO International Agency for Research on Cancer. He was elected Honorary Member of the Academy of Science of Hungary and a Member of the European Cancer Academy.

7 Acknowledgements

7.1 Conflict of interest

No conflict of interest.

7.2 Funding sources

This research did not receive any specific grant from funding agencies in the public, commercial, or not-for-profit sectors.

References

Abramoff, M.D., Folk, J.C., Han, D.P., Walker, J.D., Williams, D.F., Russell, S.R., Massin, P., Cochener, B., Gain, P., Tang, L., Lamard, M., Moga, D.C., Quellec, G., Niemeijer, M., 2013. Automated analysis of retinal images for detection of referable diabetic retinopathy. JAMA Ophthalmol 131, 351-357.

Adal, K.M., Ensing, R.M., Couvert, R., van Etten, P., Martinez, J.P., Vermeer, K.A., van Vliet, L.J., 2014. A Hierarchical Coarse-to-Fine Approach for Fundus Image Registration, In: Springer (Ed.), Biomedical image registration, London.

Bonnans, J.F., Gilbert, J.C., Lemaréchal, C., Sagastizabal, C.A., 2006. Numerical optimization. Theoretical and practical aspects, Berlin Heidelberg.

Can, A., Stewart, C.V., Roysam, B., Tanenbaum, H.L., 2002. A feature-based, robust, hierarchical algorithm for registering pairs of images of the curved human retina. IEEE Transactions on Pattern Analysis and Machine Intelligence 24, 347-364.

Cattin, P.C., Bay, H., Van Gool, L., Székely, G., 2006. Retina Mosaicing Using Local Features, In: Larsen, R., Nielsen, M., Sporring, J. (Eds.), Medical Image Computing and Computer-Assisted Intervention – MICCAI 2006. Springer Berlin Heidelberg, Zurich, Zwitserland, pp. 185-192.

Chanwimaluang, T., Fan, G., Fransen, S.R., 2006. Hybrid retinal image registration. IEEE Trans Inf Technol Biomed 10, 129-142.

Cideciyan, A.V., 1995. Registration of ocular fundus images: an algorithm using cross-correlation of triple invariant image descriptors. IEEE Engineering in Medicine and Biology Magazine 14, 52-58.

Decencière, E., Cazuguel, G., Zhang, X., Thibault, G., Klein, J.C., Meyer, F., Marcotegui, B., Quellec, G., Lamard, M., Danno, R., Elie, D., Massin, P., Viktor, Z., Erginay, A., Laÿ, B., Chabouis, A., 2013. TeleOphta: Machine learning and image processing methods for teleophthalmology. Irbm 34, 196-203.

Fang, B., Tang, Y.Y., 2006. Elastic registration for retinal images based on reconstructed vascular trees. IEEE Trans Biomed Eng 53, 1183-1187.

Fitzgibbon, A.W., 2001. Simultaneous linear estimation of multiple view geometry and lens distortion. Computer Vision and Pattern Recognition. Proceedings of the 2001 IEEE Computer Society Conference 1, I-125-I-132.

Fleming, A.D., Goatman, K.A., Philip, S., Prescott, G.J., Sharp, P.F., Olson, J.A., 2010. Automated grading for diabetic retinopathy: a large-scale audit using arbitration by clinical experts. Br J Ophthalmol 94, 1606-1610.

Harding, S., Greenwood, R., Aldington, S., Gibson, J., Owens, D., Taylor, R., Kohner, E., Scanlon, P., Leese, G., 2003. Grading and disease management in national screening for diabetic retinopathy in England and Wales. Diabet Med 20, 965-971.

Hartley, R., Zisserman, A., 2004. Multiple view geometry in computor vision. Cambridge University Press.

Lee, S., Abràmoff, M.D., Reinhardt, J.M., 2007. Feature-based pairwise retinal image registration by radial distortion correction. Proc of SPIE 6512, 651220-651220-651210.

Lee, S., Abràmoff, M.D., Reinhardt, J.M., 2008. Retinal image mosaicing using the radial distortion correction model. Proc. of SPIE 6914, 691435-691435-691439.

Lee, S., Reinhardt, J.M., Cattin, P.C., Abramoff, M.D., 2010. Objective and expert-independent validation of retinal image registration algorithms by a projective imaging distortion model. Med Image Anal 14, 539-549.

Lowe, D.G., 2004. Distinctive Image Features from Scale-Invariant Keypoints.

Matsopoulos, G.K., Mouravliansky, N.A., Delibasis, K.K., Nikita, K.S., 1999. Automatic Retinal Image Registration Scheme Using Global Optimization Techniques. IEEE Transactions on Information Technology in Biomedicine 3, 47-60.

More, J.J., 1977. Levenberg--Marquardt algorithm: implementation and theory, In: Watson, G.A. (Ed.), Numerical Analysis. Springer Verlag, United Kingdom, pp. 105-116.

Moré, J.J., 1983. Recent Developments in Algorithms and Software for Trust Region Methods, In: Bachem, A., Korte, B., Grötsche, M. (Eds.), Mathematical Programming The State of the Art. Springer Berlin Heidelberg, pp. 258-287.

Noyel, G., Jourlin, M., Thomas, R., Bhakta, G., Crowder, A., Owens, D., Boyle, P., 2015. Contrast enhancement of eye fundus images, IDF 2015, Vancouver.
Park, J., Byun, S.-C., Lee, B.-U., 2009. Lens distortion correction using ideal image coordinates. IEEE Transactions on Consumer Electronics 55, 987-991.
Quellec, G., Lamard, M., Erginay, A., Chabouis, A., Massin, P., Cochener, B., Cazuguel, G., 2016. Automatic detection of referral patients due to retinal pathologies through data mining. Med Image Anal 29, 47-64.
Ritter, N., Owens, R., Cooper, J., Eikelboom, R.H., van Saarloos, P.P., 1999. Registration of Stereo and Temporal Images of the Retina. IEEE Trans Med Imaging 18, 404-418.
Scanlon, P.H., Wilkinson, C.P., Aldington, S.J., Matthews, D.R., 2009. A practical manual of diabetic retinopathy management. Wiley Online Library.
Stewart, C.V., Tsai, C.L., Roysam, B., 2003. The dual-bootstrap iterative closest point algorithm with application to retinal image registration. IEEE Trans Med Imaging 22, 1379-1394.
Thomas, R.L., Dunstan, F., Luzio, S.D., Roy Chowdury, S., Hale, S.L., North, R.V., Gibbins, R.L., Owens, D.R., 2012. Incidence of diabetic retinopathy in people with type 2 diabetes mellitus attending the Diabetic Retinopathy Screening Service for Wales: retrospective analysis. BMJ 344, e874.
Vedaldi, A., Fulkerson, B., 2008. VLFEat: An open and portable library of computor vision algorithms. http://www.vlfeat.org/.
Walter, T., 2003. Application de la morphologie mathématique au diagnostic de la rétinopathie diabétique à partir d'images couleur. Ecole Nationale Supérieure des Mines de Paris, Paris, France.
Walter, T., Klein, J.-C., 2005. Automatic Analysis of Color Fundus Photographs and Its Application to the Diagnosis of Diabetic Retinopathy, In: Suri, J.S., Wilson, D.L., Laxminarayan, S. (Eds.), Handbook of Biomedical Image Analysis, pp. 315-368.
Wolberg, G., 1990. Digital image warping. Wiley-IEEE Computer Society Press.
Wonpil, Y., 2003. An embedded camera lens distortion correction method for mobile computing applications. IEEE Transactions on Consumer Electronics 49, 894-901.
You, X., Fang, B., He, Z., Tang, Y.Y., 2005. A Global-to-Local Matching Strategy for Registering Retinal Fundus Images, In: Marques, J.S., de la Blanca, N.P., Pina, P. (Eds.), Pattern Recognition and Image Analysis. Springer Berlin Heidelberg, China, pp. 259-267.
Zana, F., Klein, J.C., 1999a. A Multimodal Registration Algorithm of Eye Fundus Images Using Vessels Detection and Hough Transform. IEEE Trans Med Imaging 18, 419-428.
Zana, F., Klein, J.C., 1999b. A registration algorithm of eye fundus images using a Bayesian hough transform. IEEE Trans Med Imaging 18, 419-428.